Veterinary and Animal Science 25 (2024) 100383

Contents lists available at ScienceDirect

Veterinary and Animal Science

journal homepage: www.elsevier.com/locate/vas

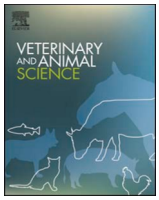

Effect of castration method on porcine skeletal muscle fiber traits and transcriptome profiles

Klavdija Poklukar [a,†], Anja Erbežnik [b,†,#], Gregor Fazarinc [b], Kevin Kress [c], Nina Batorek-Lukač [a], Martin Škrlep [a], Volker Stefanski [c], Marjeta Čandek-Potokar [a,d], Milka Vrecl [b,*]

[a] Agricultural Institute of Slovenia (KIS), Hacquetova ulica 17, SI-1000, Ljubljana, Slovenia
[b] Institute of Preclinical Sciences, Veterinary Faculty, University of Ljubljana, Gerbičeva ulica 60, SI-1000, Ljubljana, Slovenia
[c] University of Hohenheim, Garbenstraße 17, 70599, Stuttgart, Germany
[d] Faculty of Agriculture and Life Sciences, University of Maribor, Pivola 10, SI-2311, Hoče, Slovenia

ARTICLE INFO

Keywords:
Pig
Skeletal muscle
Longissimus dorsi
Semispinalis capitis
Castration method
Gene expression

ABSTRACT

This study examined the effects of immunocastration and surgical castration on the histomorphometric and transcriptome traits of the porcine skeletal muscle. We hypothesized that the differences in duration of androgen deprivation resulting from different castration methods influence skeletal muscle biology in a muscle-specific manner. This was tested by analyzing samples of m. longissimus dorsi (LD) and m. semispinalis capitis (SSC) from immunocastrated (IC; $n = 12$), entire male (EM; $n = 12$), and surgically castrated (SC; $n = 12$) pigs using enzyme/immunohistochemical classification and histomorphometric analysis of myofibers, quantitative PCR, and RNA sequencing. The results confirmed the distinctive histomorphometric profiles of LD and SSC and the castration method related muscle-specific effects at the histomorphometric and transcriptome levels. Long-term androgen deficiency (surgical castration) significantly reduced the proportion of fast-twitch type IIa myofibers in LD ($P < 0.05$), whereas short-term androgen deprivation (immunocastration) reduced the cross-sectional area of oxidative type I myofibers in SSC ($P < 0.05$). At the transcriptional level, glycolytic LD adapted to long- and short-term androgen deprivation by upregulating genes controlling myoblast proliferation and differentiation to maintain fiber size. In contrast, increased protein degradation through the ubiquitin ligase-mediated atrophy pathway (significantly increased *TRIM63* and *FBXO32* expression; $P < 0.05$) could underly reduced cross-sectional area of type I myofibers in the oxidative SSC in IC. Potential candidate genes (*HK2, ARID5B, SERPINE1*, and *SCD*) linked to specific metabolic profiles and meat quality traits were also identified in IC, providing a foundation for studying the effects of immunocastration on skeletal muscle fiber and carcass/meat quality traits.

Abbreviations: ACC, acetyl CoA carboxylase; ACTB, actin beta; AMPK, 5′-adenosine monophosphate-activated protein kinase; ANKRD1, ankyrin repeat domain 11; AR, androgen receptor; ARID5B, AT-rich interaction domain 5B; ATF3, activating transcription factor 3; BTG2, BTG anti-proliferation factor 2; CEBPB, CCAAT/enhancer-binding protein-β; CRYAB, crystallin alpha B; CSA, cross-sectional area; Ct, threshold cycle; DEGs, differentially expressed genes; ECM, extracellular matrix; EGR1, early growth response 1; EM, entire male; ER, estrogen receptor; FAS, fatty acid synthase; FBX32, F-box protein 32; FOXO1, forkhead box protein O1; GnRH, gonadotropin–releasing hormone; GO, gene ontology; GYG, glycogenin; GYS, glycogen synthase; Gα13, G-protein α-subunit 13; HK, hexokinase; IC, immunocastrated; IGF-1, insulin-like growth factor-1; IMF, intramuscular fat; JUNB, JunB proto-oncogene; KEGG, Kyoto encyclopedia of genes and genomes; LD, m. longissimus dorsi; LPL, lipoprotein lipase; MyHC, myosin heavy chain; MYOC: myoclin, NR4A3, nuclear receptor subfamily 4 group A member 3; PFK, phosphofructokinase; PPARγ, peroxisome proliferator-activated receptor gamma; PGC-1α, PPARγ coactivator 1 alpha; PRKAG2, protein kinase AMP-activated gamma 2 non-catalytic subunit; qPCR, quantitative PCR; RMSE, root-mean-square error; RNA-Seq, RNA sequencing; SC, surgically castrated; SCD, stearoyl-CoA desaturase; SDH, succinate dehydrogenase; SERPINE1, serpin peptidase inhibitor; SPP1, secreted phosphoprotein 1; SSC, m. semispinalis capitis; THBS1, thrombospondin 1; TRIM63, tripartite motif containing 63; 18S rRNA, eukaryotic ribosomal (r) 18S RNA.

* Corresponding author.
E-mail address: milka.vrecl@vf.uni-lj.si (M. Vrecl).
† These authors contributed equally to this paper.
# Current address: Institute of Microbiology and Immunology, Faculty of Medicine, University of Ljubljana, Zaloška cesta 4, SI-1000 Ljubljana, Slovenia.

https://doi.org/10.1016/j.vas.2024.100383

Available online 26 July 2024

1. Introduction

Immunocastration/vaccination against boar taint is emerging as a viable alternative to conventional surgical castration, with potential socioeconomic, environmental, and animal welfare benefits. However, concerns regarding food safety (residues), attitudes towards hormones and vaccines, and low acceptance among farmers and processors still remain (Aluwé et al., 2020; Morgan et al., 2019; Steybe, Kress, Schmucker & Stefanski, 2021). The recommended two-dose vaccination scheme against gonadotropin-releasing hormone (GnRH) triggers the production of anti-GnRH antibodies, testis regression, and reduced steroid production, thereby delaying puberty and reducing male aggressiveness and boar taint occurrence (Batorek, Čandek-Potokar, Bonneau & Van Milgen, 2012). Studies comparing growth performance, carcass value, and overall pork/meat product quality have shown that immunocastrated (IC) males tend to exhibit i) feed efficiency and carcass quality between those of surgical castrates (SC) and entire males (EM); ii) meat quality similar to that of SC; and iii) rapid fat accumulation due to the metabolism switch between the typical EM lean phenotype and fattier one characteristic of SC (Batorek et al., 2012; Bonneau & Weiler, 2019; Pauly, Luginbühl, Ampuero & Bee, 2012; Škrlep et al., 2020). In contrast, the effects of immunocastration on skeletal muscle myofibers, particularly regarding gene expression related to their contractile and metabolic properties, have been less studied.

The myofiber type composition determines the physiological, functional, and morphological properties of muscles, significantly affecting growth performance and carcass/meat quality traits (Matarneh, Silva & Gerrard, 2021; Men, Deng, Xu, Tao & Qi, 2013). The contractile properties of myofiber types (slow-twitch type I and fast-twitch types IIa, IIx, and IIb) are primarily determined by myosin heavy chain (MyHC) isoforms (I, IIa, IIx, and IIb) expressed in large porcine muscles (Lefaucheur, Milan, Ecolan & Le Callennec, 2004; Pellegrino et al., 2003). Conversely, their metabolic properties correspond to their energy requirements during contraction; types I and IIa have greater oxidative capacity, IIb is glycolytic, and IIx is metabolically intermediate (oxidative–glycolytic) (Lefaucheur, Ecolan, Plantard & Gueguen, 2002). Morphologically, oxidative myofibers tend to have a smaller cross-sectional area (CSA); however, myofiber diameter can vary depending on the muscle and its architecture (e.g. parallel, pennate) (Listrat et al., 2016; Park et al., 2022). A higher proportion of oxidative myofibers may contribute to meat quality traits including higher pH, redness, tenderness, and water-holding capacity (Men et al., 2013; Park et al., 2022). Similarly, the expression of genes involved in lipid metabolism is correlated with the proportion of intramuscular fat (IMF) (Zhang et al., 2015). Key genes include peroxisome proliferator-activated receptor gamma *(PPARγ)*, PPARγ coactivator 1 alpha *(PGC-1α)*, and lipoprotein lipase *(LPL)* (Erkens et al., 2006; Lin et al., 2002, 2014). Recently, G-protein α-subunit 13 (*Gα13*) has also been highlighted for its specific silencing, which leads to an oxidative phenotype in skeletal muscle and increase in fatty acid metabolism (Koo et al., 2017).

The contractile and metabolic phenotypes of myofibers are altered by various factors such as selective breeding, rearing conditions, diet, physical activity, and sex (reviewed in Listrat et al. (2016)). In particular, skeletal muscle is sensitive to sex steroids, so its myofiber-type composition and contractile function can be altered by the presence/absence (deficiency) of hormones (Haizlip, Harrison & Leinwand, 2015). Skeletal muscles predominantly express receptors for androgens (AR) and estrogens (ER) in satellite cells (Sinha-Hikim, Taylor, Gonzalez-Cadavid, Zheng & Bhasin, 2004). While these are abundant in myofibers with high oxidative potential (van Wessel, de Haan, van der Laarse & Jaspers, 2010), the expression of ER subtypes in the skeletal muscle of pigs is extremely low (Kalbe, Mau, Wollenhaupt & Rehfeldt, 2007). Androgen action in the skeletal muscle exerts genomic and non-genomic effects on proliferation, differentiation, and metabolism (Dubois et al., 2014; Kraemer et al., 2020; Seo et al., 2019). The anabolic effect of androgens—that is, increased skeletal muscle mass (measured as lean meat content) and myofiber size (increased CSA) is at least partly regulated by phosphatidylinositol-3-kinase/Akt signaling (Dubois, Laurent, Boonen, Vanderschueren & Claessens, 2012), but their effect on contractile function is minimal. Administration of anabolic steroids increases muscle size mostly through myofiber hypertrophy and, to a lesser extent, via new myofiber formation through the activation of satellite cells (Eriksson, Kadi, Malm & Thornell, 2005). Conversely, hypogonadism accompanied by low serum testosterone levels reduces the skeletal muscle oxidative capacity (Rossetti & Gordon, 2017). Porcine satellite cells are direct targets of androgen action, as demonstrated by the testosterone-induced upregulation of AR and satellite cell proliferation in vitro (Doumit, Cook & Merkel, 1996) and in SC neonatal pigs (Mulvaney, Marple & Merkel, 1988). Notably, increased androgens at puberty initiate their transition from a proliferative to a quiescent state (Seo et al., 2019).

Compared with SC pigs castrated in the first week after birth, the duration of androgen deprivation in IC pigs is relatively short (4–6 weeks), only occurring after the second vaccination (Kress et al., 2020). This suggests the existence of distinct and muscle type-specific effects of immunocastration on skeletal muscle. To test these assumptions, this study analyzed the histomorphometric and transcriptome profiles of two skeletal muscles with distinct architecture and contractile/metabolic characteristics, m. longissimus dorsi (LD) and m. semispinalis capitis (SSC), in EM, SC and IC pigs.

2. Materials and methods

2.1. Animals, sampling, and meat quality assessment

Muscle samples for the trial were derived from one processing batch ($n = 36$) of a previously described experiment (Kress et al., 2020) (approval ID HOH 47/17TH; Ethical committee for animal experiments of the regional authority of Tübingen, Germany). Commercial crossbreeds (Landrace × Pietrain crosses) were assigned to three sex categories: EM ($n = 12$), SC ($n = 12$), and IC ($n = 12$). Piglets from the SC group were surgically castrated within the first week of life. IC pigs were vaccinated against GnRH using the IMPROVAC vaccine (Zoetis Deutschland GmbH, Berlin, Germany) twice, at 12 and 21.5 weeks. The vaccination success in IC was 100% and was previously confirmed; the testicular function in IC was efficiently suppressed and boar taint was prevented (Batorek-Lukač et al., 2022; Fazarinc et al., 2023; Kress et al., 2020). During rearing, all animals were fed ad libitum with the same commercial diet. Animals were processed in one batch at the age of 27.5 weeks according to routine abattoir procedures (CO_2 stunning, scalding, evisceration). At the end of the processing line (45 min postmortem), ~1 cm^3 muscle samples were collected from the central part of the LD at the level of the last rib and from the SSC (the central part of the m. biventer cervicis) at the level of the fourth cervical vertebra. Muscles were sampled from the right side of the carcass, snap-frozen in liquid nitrogen, and stored at −80 °C until subsequent analysis. Information on the live weights and carcass traits of the animals included in the study is summarized in Table S1.

2.2. Enzyme-/immunohistochemistry and histomorphometric analysis

The myofiber types in LD and SSC were classified as previously described (Fazarinc et al., 2017, 2020). Transverse serial cryosections (10 μm) of LD and SSC were used for enzyme-/immunohistochemistry. The mitochondrial SDH activity was used to assess the oxidative potential of the myofibers (Nachlas, Tsou, de Souza, Cheng & Seligman, 1957). For immunohistochemistry, two different monoclonal antibodies (MAb) specific for adult MyHC isoforms were used: NLC-MHCs (slow; Novocastra laboratories, Newcastle in Tyne, UK) specific for slow-twitch MyHC I, and SC 71 specific for MyHC IIa (Schiaffino et al., 1989) (Fig. 1A). The immunohistochemistry protocol was as previously

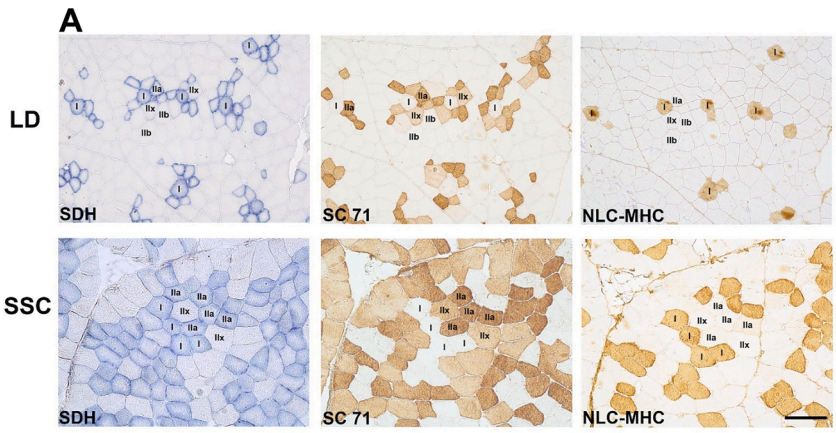

B

	Myofiber type			
	I	IIa	IIx	IIb
SDH	++	++/+	+/–	–
SC 71	–	++	+	–
NLC-MHCs (slow)	++	–	–	–

++ strong positive reaction; ++/+ strong/moderate positive reaction; + moderate positive reaction; +/– moderate/negative reaction; – negative reaction.

Fig. 1. Enzyme-/immunohistochemistry-based myofiber classification in the m. longissimus dorsi (LD) and m. semispinalis capitis (SSC). (A) Transverse sections of LD (upper panels) and SSC (lower panels) were analyzed for succinate dehydrogenase (SDH) activity, demonstrating the oxidative profile of myofibers, and stained with the monoclonal antibodies SC 71 and NLC-MHCs (slow) specific for myofiber types IIa/IIx and I, respectively. Scale bar: 200 μM. **(B)** Summary of myofiber types I, IIa, IIx, and IIb classification based on the succinate dehydrogenase (SDH) activity and specificity of utilized primary antibodies.

described (Fazarinc et al., 2017, 2020). A Nikon Eclipse Ni-UM microscope equipped with a DS-Fi1 camera and the Imaging Software NIS-Elements BR 4.60 (Nikon Instruments Europe B.V., Badhoevedorp, The Netherlands) were used for myofiber classification and histomorphometric analysis, performed as described in a previous study (Fazarinc et al., 2020), as well as for quantitative assessment of SDH staining intensity. The classification of individual myofiber types (I, IIa, IIx, and IIb) based on the SDH staining intensity and immunohistochemical results is summarized in Fig. 1B. The intensity of SDH staining was quantitatively assessed by measuring the mean brightness of the SDH-stained myofiber types. Mean brightness values are inversely proportional to SDH staining activity, and are the lowest for type 1 and highest for IIb/IIx myofibers. The CSA (μm^2) of individual myofiber types was also measured and the myofiber relative area was calculated using the following equation.

$$Myofiber\ relative\ area\ (\%) = \frac{myofiber\ CSA\ x\ proportion\ of\ myofiber\ type}{average\ CSA\ of\ all\ myofiber\ types} \quad (1)$$

2.3. RNA isolation

RNA isolation, cDNA synthesis, and qPCR were performed as previously described (Vrecl, Cotman, Uršič, Čandek-Potokar, & Fazarinc, 2018). Total RNA from ~25 mg snap-frozen muscle samples was extracted using the RNeasy Fibrous Tissue Mini Kit (Qiagen, Stockach, Germany). The extraction protocol included an on-column DNase digestion step with RNase-Free DNase Set; (Qiagen). Absorbance ratios (260/280 and 260/230) were determined using an ultraviolet–visible (UV–VIS) Lambda 25 spectrophotometer (Perkin Elmer, Waltham, MA, USA) to check for potential contamination. The integrity and quality of the RNA samples was controlled by Qubit RNA IQ assay using Invitrogen™ Qubit™ 4 Fluorometer. The RNA integrity number of all RNA samples was higher than 6.3. Isolated RNA samples were used for qPCR and RNA-seq.

2.4. cDNA synthesis and quantitative polymerase chain reaction (qPCR)

RT^2 First Strand Kit (Qiagen) was used for cDNA synthesis from one microgram of each RNA sample. Primers and fluorescent 6-FAM dye-labeled minor groove binder probes/predesigned assays were from Applied Biosystems (Thermo Scientific GmbH, Vienna, Austria). The primers/probes used to detect *MyHC* isoforms I, IIa, IIx, and IIb, were as reported previously (Vrecl et al., 2018). The Custom TaqMan® Assay Design Tool was used to design primers/probes for the pig *Gα13* gene using predicted Sus scrofa G protein subunit alpha 13 mRNA as an input sequence (NCBI Reference Sequence: XM_003357998.4). The sequences of primer pairs and probes to detect *Gα13* were: 5-GCAGACAGTGGCA-TACAGAATG (forward); 5-CTCCAAGTTTATCCAAGTTATCCAGGAAA (reverse); and 5- TCACCCAACTGAAATTC (probe). The assays used in this study are listed in Table S2. Eukaryotic ribosomal (r) *18S* RNA (*18S* rRNA) and *actin beta* (*ACTB*) were used as endogenous controls; their suitability for the qPCR data normalization of LD samples in pigs was previously reported (Erkens et al., 2006; Wimmers et al., 2008). qPCR utilized a 10 μL reaction volume consisting of 4.5 μL of the 10-fold diluted cDNA and 5.5 μL of the TaqMan universal PCR Master Mix using the QuantStudio™ 5 Real-Time PCR System (ThermoFisher Scientific, Applied Biosystems, Foster City, CA, USA) under the following conditions: one cycle of 50 °C for 2 min and one cycle of 95 °C for 10 min, followed by 45 cycles of 15 s at 95 °C and 1 min at 60 °C. Each reaction was performed in triplicate. The results were calculated from the threshold cycle (Ct) that was fixed at 0.10. A Ct value > 35 was regarded as the cutoff. The comparative Ct method (ΔCt = Ct geometric mean of controls – Ct target transcript) was used for relative quantification of target transcripts normalized against the geometric mean of 18S rRNA and ACTB. The relative changes in the expression of the studied target transcripts (fold changes in the expression) were compared between LD and SSC and between sex categories within LD and SSC using the $2^{\Delta\Delta Ct}$ method. The PCR (>90%) efficiency of the studied genes was derived from standard curves composed of four 10-fold dilutions of cDNAs. Data analysis was performed with Applied

Table 1
Distinctive characteristics of m. longissimus dorsi (LD) and m. semispinalis capitis (SSC).

	Muscle type		
	LD	SSC	*P*-value
Chemical composition			
IMF (%)	1.65 ± 0.61	7.07 ± 1.56	<0.001
Moisture (%)	73.65 ± 0.79	72.01 ± 1.62	<0.001
Proteins (%)	24.62 ± 0.63	20.49 ± 0.91	<0.001
Myofiber type (%)			
Type I	8.69 ± 2.17	38.65 ± 6.34	<0.001
Type IIa	10.63 ± 3.05	34.14 ± 4.37	<0.001
Type IIx	16.65 ± 5.35	27.21± 3.86	<0.001
Type IIb	64.03 ± 8.02	–	–
SDH ++	19.32 ± 4.03	72.84 ± 3.96	<0.001
CSA (μm^2)			
Type I	3777 ± 889	7216 ± 1214	<0.001
Type IIa	2998 ± 591	6046 ± 1600	<0.001
Type IIx	5797 ± 1192	7370 ± 2032	<0.001
Type IIb	7609 ± 1486	–	–
All fibers	6464 ± 1133	6868 ± 1157	*ns*
Myofiber relative area (%)			
Type I	5.16 ± 1.77	40.80 ± 7.73	<0.001
Type IIa	5.04 ± 1.76	30.01 ± 5.66	<0.001
Type IIx	15.04 ± 5.44	29.18 ± 5.70	<0.001
Type IIb	74.76 ± 7.41	–	–

Data are represented as mean ± SD; $n = 36$ per muscle. LD: m. longissimus dorsi; SSC: m. semispinalis capitis; IMF: intramuscular fat content; CSA: cross-sectional area; SDH ++: succinate dehydrogenase positive myofibers; –: not detected; *ns*: not significant (Student's *t*-test; $P > 0.05$).

Biosystems™ Analysis Software (Relative Quantification Analysis Module, version 3.9).

2.5. cDNA library preparation and RNA-sequencing (RNA-seq)

RNA-Seq was performed to compare the effects of sex on transcript expression (differential gene expression) in LD and SSC, as previously described for adipose tissue (Poklukar et al., 2021). Briefly, equal amounts of extracted RNA from six randomly selected animals of each sex category and muscle were pooled and used for library preparation and sequencing. The decision to utilize one pooled RNA sample per muscle and sex category was made to optimize the cost of the experiment without a significant loss of power in differentially expressed gene (DEG) analysis (Ko & Van Raamsdonk, 2023). A total of 3 µg of pooled RNA was used for generating sequencing libraries using the NEBNext Ultra RNA Library Preparation Kit for Illumina (NEB, Ipswich, MA, USA). Library concentrations were quantified using the Agilent Bioanalyzer 2100 System (Agilent, Santa Clara, CA, USA). After clustering index-coded samples on a cBot Cluster Generation System (Illumina, San Diego, CA, USA), cDNA libraries were sequenced on an Illumina HiSeq 2500 generating 150 bp paired-end reads (Novogene Bioinformatics Technology Co., Ltd., Beijing, China). The RNA-Seq experiment was submitted to the NCBI Gene Expression Omnibus (GEO; Bethesda, MD, USA) and assigned the GEO accession number GSE183240.

2.6. RNA-Seq data - quality control, mapping, and assembly

Raw sequencing data were obtained from Novogene Bioinformatics Technology Co., Ltd. Quality control analysis data for each sequenced library is shown in Table S3. Using in-house Perl scripts, reads with adaptor contamination, more than 10% uncertain nucleotides, and reads with poor-quality nucleotides (base quality less than 20) were discarded. The error rate (%), quality scores (Q20 and Q30), and guanine-cytosine (GC) content (%) of the resulting high-quality clean reads were evaluated. Clean reads were then aligned to the reference genome Sscrofa10.2 (Genbank assembly GCA_000003025.6) using TopHat2 v2.0.12 and Bowtie v2.2.3, with default parameters allowing up to two base mismatches. The read counts were adjusted using the edgeR program package with a scaling normalization factor. DEG analysis was performed by comparing the two groups in each muscle (EM vs. IC, IC vs. SC, and EM vs. SC) using the DEGSeq R package (version 1.20.0). The resulting *P*-values were adjusted using the Benjamini–Hochberg method. The threshold for significant differential expression was set to a corrected Q value of 0.005 and |log2 (fold change)| of 1. The selected set of DEGs was verified using qPCR, as described above. A volcano plot was constructed using the Enhanced Volcano R package v. 1.8.0.

2.7. Functional enrichment analysis

Gene Ontology (GO) over-representation analysis of DEGs was performed using the R package GOSeq (Young, Wakefield, Smyth & Oshlack, 2010) and included a correction for gene lengths. GO terms with corrected *P*-values < 0.05 were considered to be significantly enriched. In addition, the Kyoto Encyclopedia of Genes and Genomes (KEGG) Orthology-Based Annotation System (KOBAS 2.0) was used to annotate and identify enriched pathways in the KEGG and to test the over-representation of DEGs in the KEGG pathways using Fisher's exact tests. The test results were subjected to multiple test *P*- value corrections using the Benjamini–Hochberg correction. The R package GOplot (Walter, Sánchez-Cabo & Ricote, 2015) was used to visually combine and integrate expression data with the results of the functional analysis.

2.8. Statistical analysis

A general linear model procedure in the SAS statistical program (SAS Institute Inc., Cary, NC, USA) was used. The model included the sex category as a fixed effect. When the differences between the least square means were significant ($P < 0.05$), the groups were compared using Tukey's adjustment. The evaluated parameter means of LD and SSC were compared using the Student's *t*-test.

Table 2
Expression of genes related to contractile and metabolic phenotypes and the receptors for androgens (*AR*) and estrogens (*ER*) of m. longissimus dorsi (LD) and m. semispinalis capitis (SSC).

	LD vs. SSC	
Target transcript	Fold change	*P*-value
MyHC-I	−7.26 (−10.44 to −5.04)	<0.0001
MyHC-IIa	−5.32 (−6.84 to −4.13)	<0.0001
MyHC-IIx	1.45 (1.12–1.86)	0.034
MyHC-IIb	1072 (758–1514)	<0.0001
PPARγ	−2.50 (−3.27 to −1.91)	0.013
PGC-1α	−9.51 (−12.72 to −7.11)	<0.0001
Gα13	−1.39 (−1.67 to −1.15)	*ns*
HK2	−4.48 (−5.95 to −3.37)	<0.0001
LPL	−3.79 (−4.69 to −3.07)	<0.0001
AR	1.44 (1.16–1.78)	*ns*
ERα	−1.25 (1.57–1.00)	*ns*

Gene expression mean fold changes with upper and lower limits for LD versus SSC. Fold-change values < 1 were substituted with a negative inverse of the original fold-change values. *MyHC*: myosin heavy chain; *PPARγ*: peroxisome proliferator-activated receptor gamma; *PGC-1α*: PPARγ coactivator 1 alpha; *Gα13*: G-protein α-subunit; *HK2*: hexokinase 2; *LPL*: lipoprotein-lipase. *AR*: androgen receptor; *ERα*: estrogen receptor 1 (ER-alfa). The upper and lower limits were calculated for each fold-change value using the standard error of the mean. ns: not significant (Student's *t*-test; $P > 0.05$).

3. Results

3.1. Characteristics of LD and SSC

Initially it was shown that studied muscles i.e., predominantly glycolytic LD and oxidative SSC display distinctive characteristics related to chemical compositions, contractile, metabolic and morphometric characteristics (Tables 1 and 2). Differences in the relative expression of genes related to the contractile (*MyHC-I*, *-IIa, IIx*, and *IIb*) and metabolic phenotype (*PGC-1α, PPARγ, LPL, HK2*, and *Gα13*) in LD and SSC summarized in Table 2 are largely in agreement with those of the enzyme-/immunohistochemical classification of myofiber types. Pure type IIb myofibers were not identified by immunohistochemical or SDH activity-based approaches in SSC, which corroborates the very low *MyHC-IIb* mRNA levels detected by qPCR (cf. Tables 1 and 2). Additional quantitative assessment revealed that fiber type-specific SDH activity was not altered in IC or SC when compared to EM, with the exception of type I myofibers from EM compared to SC in SSC (Table S4). Expression levels of *AR* and *ERα* were comparable in both muscles (Table 2), whereas the expression of *ERβ* was below the detection limit (data not shown).

3.2. Effect of sex category on chemical composition, myofiber type profile, and histomorphometric characteristics of LD and SSC

The effect of the male sex on the studied characteristics is shown in Table 3. Significant differences were observed between the EM and SC groups. Water and protein contents in LD significantly varied between EM and SC ($P < 0.05$). In SSC, the IMF content was significantly lower in EM than in SC ($P = 0.030$), whereas the water content in SSC was substantially higher than in SC or IC ($P = 0.001$). Histomorphometric assessments also revealed sex category- and muscle-related effects on individual parameters. The effect on the myofiber type profile was only in LD because the percentage of type IIa myofibers significantly differed between EM and SC ($P = 0.018$) but neither category differed from IC. In SSC, IC had significantly decreased the CSA of type I myofibers compared with EM or SC ($P = 0.003$). Concomitantly, significant differences were observed in the relative areas of types I and IIa myofibers. The relative area occupied by type I myofibers was significantly lower and that of type IIa myofibers was higher in SSC in IC than in EM ($P \leq 0.05$).

3.3. Effect of the male sex category on the relative expression of selected genes related to the contractile and metabolic phenotype of LD and SSC

We observed no significant effect of the male sex on the relative expression of preselected genes related to the contractile and metabolic phenotypes of LD and SSC ($P \geq 0.05$), except for HK2 (Fig. 2). Upon short-term androgen deprivation by immunocastration, the mRNA expression of the glycolytic enzyme *HK2* was around 2-fold higher in the SSC of IC than in the SSC of SC ($P < 0.05$). The *PGC-1α* expression in the SSC was increased in EM and IC compared with in SC, but the differences

Table 3
Characteristics of the m. longissimus dorsi (LD) and m. semispinalis capitis (SSC) muscles according to the male sex category.

	LD					SSC				
	EM	IC	SC	RMSE	*P*-value	EM	IC	SC	RMSE	*P*-value
Chemical composition										
IMF (%)	1.4	1.7	1.8	0.61	0.286	6.1^{a}	7.4^{ab}	7.7^{b}	1.44	0.030
Moisture (%)	74.2^{b}	73.6^{ab}	73.2^{a}	0.68	0.004	73.3^{b}	71.6^{a}	71.1^{a}	1.35	0.001
Proteins (%)	24.2^{a}	24.8^{ab}	24.8^{b}	0.57	0.021	20.4	20.7	20.3	0.92	0.564
Myofiber type (%)										
Type I	9.3	8.0	8.8	2.16	0.319	41.0	37.9	37.2	6.42	0.323
Type IIa	12.1^{b}	11.0^{ab}	8.8^{a}	2.78	0.018	32.6	34.8	35.0	4.32	0.342
Type IIx	17.3	17.9	14.8	5.32	0.320	26.40	27.3	27.8	4.03	0.693
Type IIb	61.3	63.1	67.7	7.77	0.130	–	–	–	–	–
SDH ++	21.4	19.0	17.5	3.80	0.052	73.6	72.7	72.2	4.03	0.693
CSA (μm^2)										
Type I	4185	3393	3754	851.6	0.089	7584^{b}	6291^{a}	7773^{b}	1044.1	0.003
Type IIa	3047	3085	2864	600.6	0.632	5706	5997	6436	1387.4	0.440
Type IIx	6194	5545	5653	1192.0	0.372	7699	7225	7187	1629.9	0.695
Type IIb	8083	7403	7342	1489.9	0.410	–	–	–	–	–
All myofibers	6721	6258	6413	1150.0	0.609	7024	6418	7162	1143.6	0.252
Myofiber relative area (%)										
Type I	6.0	4.3	5.1	1.67	0.065	44.7^{b}	37.1^{a}	40.6^{ab}	7.28	0.050
Type IIa	5.5	5.5	4.1	1.68	0.080	26.4^{a}	32.3^{b}	31.4^{ab}	5.15	0.017
Type IIx	15.9	15.8	13.4	5.48	0.469	29.0	30.6	28.0	5.76	0.533
Type IIb	72.6	74.4	77.3	7.36	0.296	–	–	–	–	–

Values are presented as least square means; RMSE: root-mean-square error; $n = 12$ per muscle in the sex category; total $n = 72$; EM: entire male; IC: immunocastrated; SC: surgically castrated; LD: longissimus dorsi muscle; SSC: semispinalis capitis muscle; IMF: intramuscular fat content; CSA: cross-sectional area; SDH ++: succinate dehydrogenase activity; –: not detected. Significant differences ($P < 0.05$) among the male sex categories within a muscle (LD or SSC) are indicated by different superscript letters (a and b).

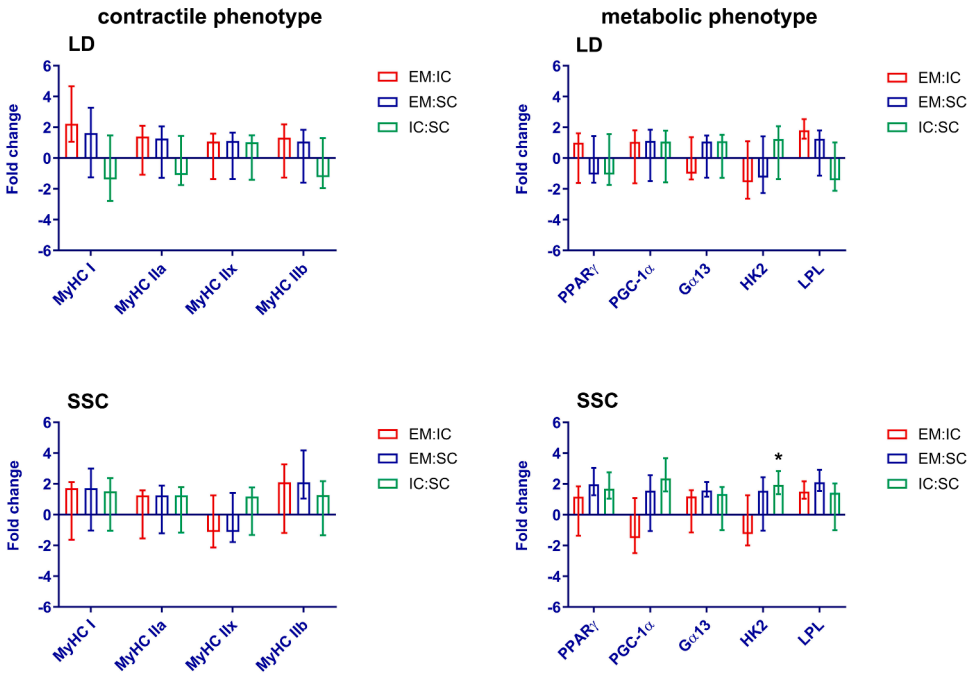

Fig. 2. Comparison of gene expression related to the contractile (left panels) and metabolic phenotype (right panels) in the m. longissimus dorsi (LD) and m. semispinalis capitis (SSC) between male sex categories. The mean fold changes are presented with upper and lower limits in the expression for EM in comparison to IC (EM:IC) and SC (EM:SC) and for IC in comparison to SC (IC:SC). A fold-change value < 1 was replaced by the negative inverse of the original fold-change value. *MyHC: myosin heavy chain; PPARγ: peroxisome proliferator-activated receptor gamma; PGC-1α: PPARγ coactivator 1 alpha; Gα13: G-protein α-subunit; HK2: hexokinase 2; LPL: lipoprotein-lipase*; EM: entire male; IC: immunocastrated; SC: surgically castrated. Upper and lower limits were calculated for each fold-change value using the standard error of the mean. *, significantly different between compared male sex categories ($P < 0.05$; Tukey's test).

were not significant ($P < 0.10$). A similar trend was observed for the enzyme involved in lipid metabolism (LPL) in EM compared with SC.

3.4. RNA-Seq data analysis of the effect of the male sex category on transcript expression in LD and SSC

We employed RNA-Seq to identify additional genes and pathways underlying histomorphometric and muscle-dependent differences between the male sex categories. Sequencing yielded 77–117 million high-quality reads for the EM, IC, and SC pools of LD and SSC (Table S5). Approximately 73%–78% of the clean reads were mapped to the annotated Sscrofa 10.2 genome. Among all mapped clean reads, more than 68.9% had unique matches and 3.9%–4.3% showed multiple-position matches (Table S5). Volcano plots (Fig. 3) showed DEGs between EM and IC, EM and SC, and IC and SC in LD and SSC. In total, 71 and 36 DEGs were detected in LD and SSC, respectively [|log2(fold-change) > 1| and -log10(q-value) < 0.005]. In LD, 36 DEGs (eight upregulated and 28 downregulated) were detected between EM and IC. Twenty-nine DEGs (10 upregulated and 19 downregulated) were detected between EM and SC. Only six DEGs (five upregulated and one downregulated) were detected when comparing IC and SC. In SSC, the number of DEGs was lower compared with that in LD. Only eight DEGs were detected when the EM and IC or EM and SC groups were compared. Interestingly, the number of DEGs between IC and SC was higher in SSC than that in LD (20 vs. 6). The complete lists of all identified DEGs and their respective fold changes and q-values for the comparison of LD and SSC categories are shown in Tables S6 and S7, respectively. Significant differences in the expressions of AR and ERα were neither detected with RNA-Seq (Tables S6 and S7) nor with qPCR (Table S8).

3.5. Expression validation of selected DEGs by qPCR

To validate the RNA-Seq results, we examined the relative expression of the selected DEGs using qPCR. Consistent with the qPCR data of initially preselected genes (Fig. 2), RNA-Seq of pooled samples revealed the upregulation of *HK2* in IC compared with SC in SSC. In addition, muscle-independent upregulation of *PGC-1α* was identified in EM and IC compared with SC, whereas qPCR on individual animals showed a similar trend in SSC but this was not significant due to the large differences between individual animals within the group.

The validation of the expression of additional DEGs by qPCR is shown in Fig. 4. Pairwise comparisons between sex categories were largely consistent with the RNA-Seq data. The results of qPCR also confirmed a higher expression of *serpin peptidase inhibitor* (*SERPINE1*) in LD in IC than in EM and SC ($P < 0.05$). The qPCR data also showed an increased expression of *tripartite motif containing 63* (*TRIM63*) in the EM compared with that in both the IC and SC ($P < 0.05$); the latter was not detected by RNA-Seq. The qPCR and RNA-Seq data for the selected DEGs were consistent in SSC. We validated the higher expressions of TRIM63 and *F-box protein 32* (*FBXO32*) in EM and IC than in SC and the lower expression of *stearoyl-CoA desaturase* (*SCD*) in EM than in SC ($P < 0.05$).

3.6. Gene ontology and KEGG pathway over-representation analysis

For the functional annotation of DEGs, GO classification and KEGG pathway over-representation analyses were performed. The results are presented in Fig. 5 and Table 4. Most of the identified enriched GO terms belong to the biological process category. The relationship between the DEGs and significantly enriched GO terms is presented in Fig. 5. The complete lists of all identified GO terms and their corresponding DEGs for comparing LD and SSC are provided in Tables S9 and S10, respectively. In LD, downregulated genes predominate in EM compared with IC and SC and are mainly related to skeletal muscle tissue development and skeletal cell differentiation (EM vs. SC) and the negative regulation of biological/cellular processes (EM vs. IC; adj. $P < 0.05$). In the comparison between IC and SC, predominantly upregulated genes were observed, and the enriched GO terms were related to various biological processes including the regulation of fibrinolysis, apoptosis, energy

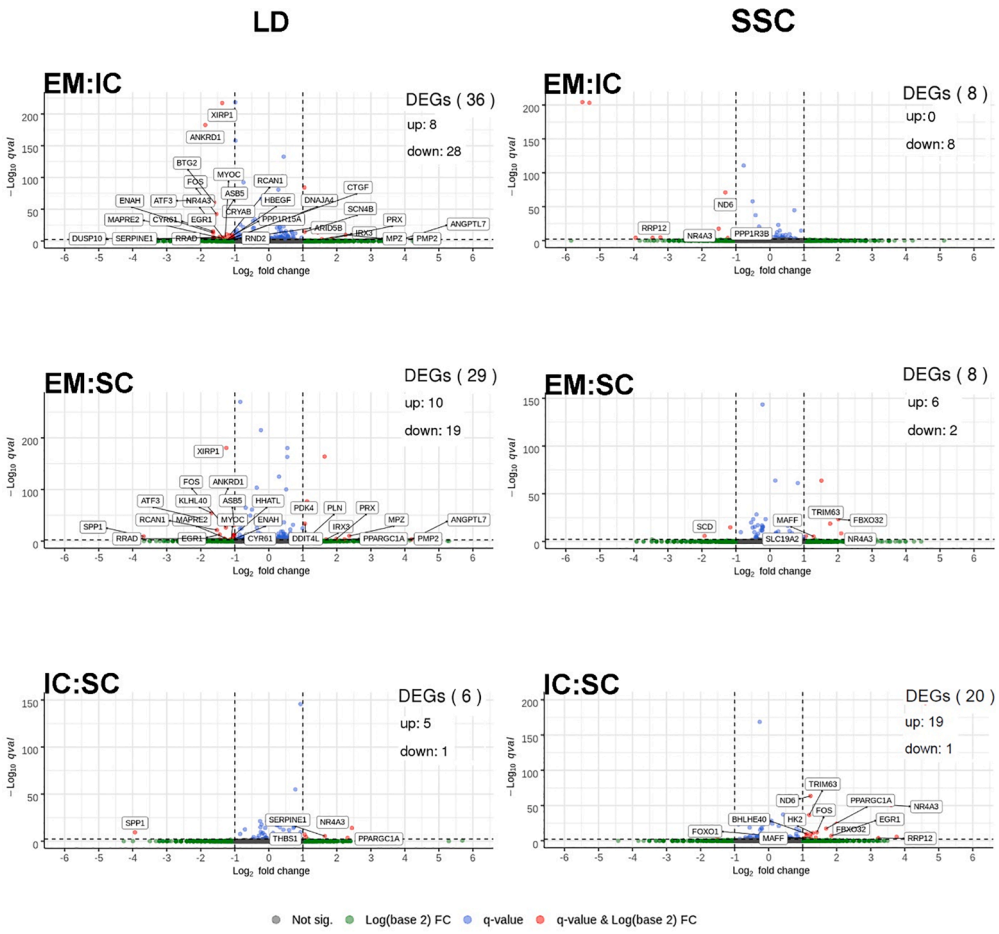

Fig. 3. Volcano plots of differentially expressed genes (DEGs) of the m. longissimus dorsi (LD) and m. semispinalis capitis (SSC) between male sex categories. Horizontal lines show the significance threshold of DEGs at -log10(q-value) < 0.005. Vertical lines represent the threshold of |log2 (fold change) >1|. Red dots represent up- and downregulated DEGs at |log2 (fold change) >1| and -log10(q-value) < 0.005. Names of selected DEGs are also displayed. Blue and green dots represent the remaining DEGs that did not meet the specified criteria. EM: entire male; IC: immunocastrated; SC: surgically castrated.

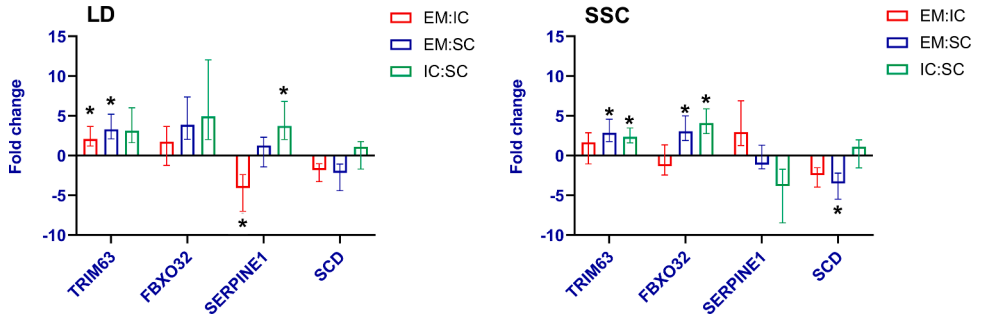

Fig. 4. Validation of selected DEGs identified by RNA-Seq in the m. longissimus dorsi (LD) and m. semispinalis capitis (SSC) between male sex categories using qPCR. The mean fold changes are presented with upper and lower limits in the expression for EM compared with IC (EM:IC) and SC (EM:SC) and for IC compared with SC (IC:SC). A fold-change value < 1 was replaced by the negative inverse of the original fold-change value. *TRIM63: tripartite motif containing 63; FBX32: F-box protein 32; SERPINE1: serpin peptidase inhibitor; SCD: stearoyl-CoA desaturase*; EM: entire male; IC: immunocastrated; SC: surgically castrated. Upper and lower limits were calculated for each fold-change value using the standard error of the mean. *, significantly different between compared male sex categories ($P < 0.05$; Tukey's test).

homeostasis, fatty acid oxidation, and behavior (adj. $P < 0.05$). In SSC, significantly enriched GO terms were only identified for predominantly upregulated genes in IC compared with SC and were associated with the regulation of energy homeostasis and fatty acid oxidation, response to hormones/stimuli, and the regulation of cellular ketone metabolic processes (see Fig. 5 and Table S10).

Significantly enriched pathways of DEGs obtained by KEGG analysis are listed in Table 4. Complete lists of all identified enriched KEGG pathways for the comparison of LD and SSC can be found in Tables S11 and S12, respectively. No significantly enriched pathways were identified in LD DEGs when EM was compared with IC or SC, whereas the IC:SC comparison showed that DEGs were enriched in p53 signaling (*thrombospondin 1* (*THBS1*), *SERPINE1* and in the extracellular matrix (ECM)-receptor interaction pathway (*THBS1, secreted phosphoprotein 1* (*SPP1*)) (adj. $P < 0.05$; see Tables 5 and S9). In SSC, DEGs in EM vs. IC, EM vs. SC, and IC vs. SC were significantly enriched in the

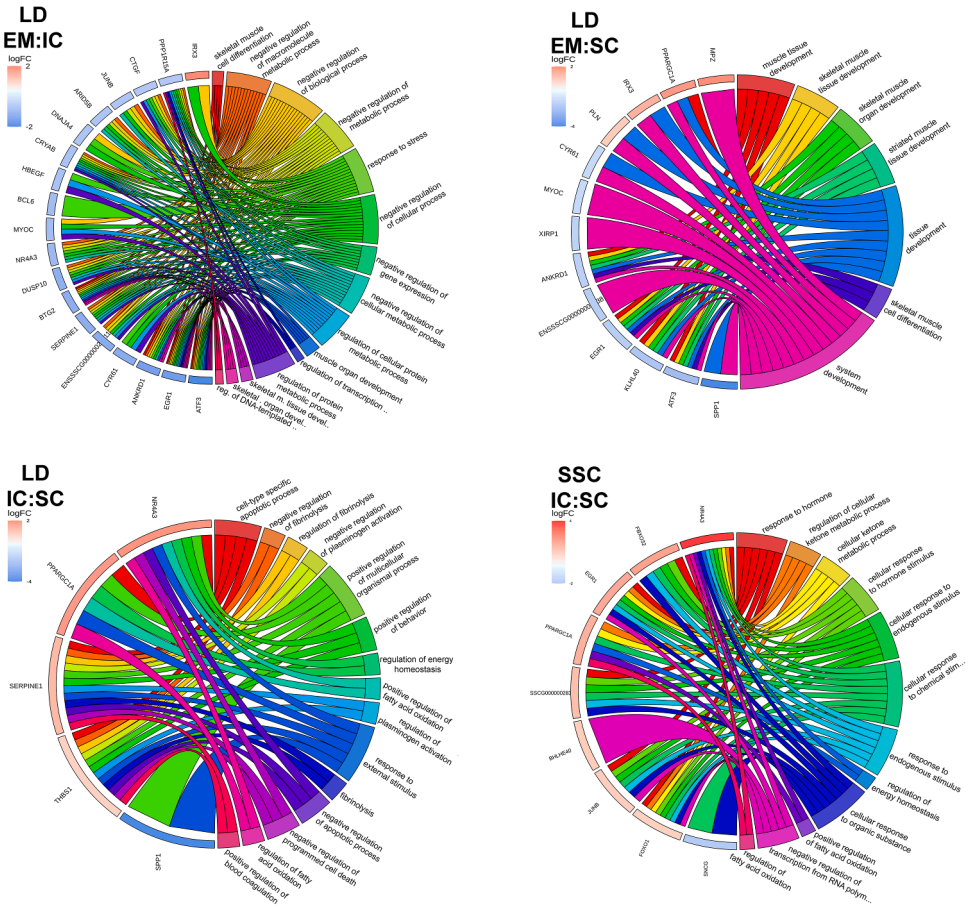

Fig. 5. GOChord plot of Gene Ontology (GO) terms enriched in the biological processes category in the m. longissimus dorsi (LD) and m. semispinalis capitis (SSC) between male sex categories. Genes are linked to their associated GO terms via colored ribbons. Genes are ordered by observed $\log_2$ fold change (logFC). The results of the functional analysis are only shown for significantly enriched GO terms. EM: entire male; IC: immunocastrated; SC: surgically castrated.

Table 4
KEGG-enriched pathways of DEGs in the m. longissimus dorsi (LD) and m. semispinalis capitis (SSC) between male sex categories.

Muscle/male sex category	Term	adj. *P*-value	Counts	Genes
LD/IC:SC	p53 signaling pathway	0.0498	2	*THBS1, SERPINE1*
LD/IC:SC	ECM-receptor interaction	0.0498	2	*THBS1, SPP1*
SSC/EM:IC	Transcriptional misregulation in cancer	0.0089	2	*NR4A3, CEBPB*
SSC/EM:SC	AMPK signaling pathway	0.0242	2	*PGC-1α, SCD*
SSC/IC:SC	Insulin signaling pathway	0.03451	4	*PGC-1α, HK2, PRKAG2, FOXO1*

THBS1: thrombospondin 1; SERPINE1: serpin peptidase inhibitor; SPP1: secreted phosphoprotein 1; NR4A3: nuclear receptor subfamily 4 group A member 3; CEBPB: CCAAT/enhancer-binding protein-β; PGC-1α: PPARγ coactivator 1 alpha; SCD: stearoyl-CoA desaturase; HK2: Hexokinase 2; PRKAG2: Protein kinase AMP-activated gamma 2 non-catalytic subunit; FOXO1: forkhead box protein O1; EM: entire male; IC: immunocastrated; SC: surgically castrated.

transcriptional misregulation in cancer (*nuclear receptor subfamily 4 group A member 3* (*NR4A3*), *CCAAT/enhancer-binding protein-β* (*CEBPB*)), 5′-adenosine monophosphate-activated protein kinase (AMPK) signaling pathway (*PGC-1α, SCD*), and insulin signaling pathway (*PGC-1α, HK2, protein kinase AMP-activated gamma 2 non-catalytic subunit (PRKAG2*), *forkhead box protein O1* (*FOXO1*)), respectively (adj. $P < 0.05$; see Tables 4 and S12).

4. Discussion

In view of the societal pressure to end piglet castration without pain relief (animal welfare issue), research into alternatives has intensified over the last decade and immunocastration has shown particular promise. However, a recent scenario analysis has shown that due to the diversity of European pork production systems, which differ in terms of animal welfare, quality, costs, product types and trade relationships (e.g. uncertainty about the acceptance of the different castration alternatives in Asian markets), all alternatives, i.e. production of entire males, immunocastration and surgical castration with pain relief, are likely to coexist in the EU (Lin-Schilstra & Ingenbleek, 2022). Regarding meat quality characteristics, it has been suggested that the differences in myofiber composition and meat quality are due to the different roles of the muscles in different positions rather than their architecture and that the meat industry should have quality control based on the physico-chemical and histological characteristics of each muscle, regardless of its architecture (Park et al., 2022). Pigs subjected to immunocastration have been extensively studied, particularly with regard to carcass and meat quality traits (Batorek et al., 2012; Bonneau & Weiler, 2019; Škrlep et al., 2020; Werner et al., 2021), the suitability of meat products (Škrlep et al., 2020), animal welfare (Bonneau & Weiler, 2019), and consumer and stakeholder attitudes (Aluwé et al., 2020; Borell et al., 2020). However, there is a notable lack of information concerning changes in

the histomorphometric characteristics and transcriptome profiles of skeletal muscles in relation to the hormonal status among different sex categories, specifically comprehensive comparisons of EM, IC, and SC. Given that a skeletal muscle is a sex steroid-sensitive tissue, this study assessed the effect of the androgen deprivation length resulting from different castration methods (immunocastration vs. surgical castration in the neonatal period) on the histomorphometric characteristics and transcriptome profiles of pig muscles with distinct architecture and contractile/metabolic profiles: unipennate glycolytic LD and multipennate oxidative SSC.

We initially confirmed unique features of the studied muscles, including differences in i) chemical composition, ii) histomorphometric myofiber profiles, and iii) expression patterns of preselected genes related to muscle contractile and metabolic phenotype, except for Gα13.

The IMF content in LD was below 2% in all tested groups, i.e. below the level required to improve the sensory properties of pork meat including palatability, juiciness and tenderness. A significantly lower protein and moisture content in SSC compared to LD corresponds to the higher IMF content (around 7% in all tested groups) in SSC (Daszkiewicz, Bąk & Denaburski, 2005). Observed differences in the proportion of individual myofiber types in LD and SSC were expected and corroborated with the results of a previous study that reported an almost five-fold higher proportion of type I myofibers in SSC than in LD (Lefaucheur et al., 1991). The proportion of fast-twitch glycolytic myofibers aligned with the histochemical enzyme classification of myofibers in LD of Pietrain × Landrace crossbred pigs (Fiedler et al., 1999), which were also used in the present study. Furthermore, the two- to threefold higher CSA of types I and IIa oxidative myofibers in SSC compared with similar myofibers in LD confirms that the size (CSA) is not solely myofiber type-dependent (Fernandez, Lefaucheur, & Čandek, 1995), and is consistent with the study showing that multipennate muscles, here exemplified by SSC, have significantly larger myofibers than muscles in the unipennate group such as LD (Park et al., 2022). We observed no effect of immunocastration on carcass characteristics or muscle chemical composition because most of these parameters differed significantly between EM and SC. These findings are consistent with the results of our previous study (Škrlep et al., 2020) and corroborate the systematic meta-analysis (Batorek et al., 2012; Pauly et al., 2012).

Differences in the hormonal (androgen) status among the studied male sex categories led to muscle-specific effects at the histomorphometric level. Compared with EM, long-term androgen deficiency resulting from surgical castration decreases the proportion of oxidative, fast-twitched type IIa myofibers in LD. This corroborates the notion that androgens support the fast-twitch phenotype in male muscles (Rana, Lee, Zajac & MacLean, 2014) and recent data obtained with fast-twitch muscle-specific AR knockouts, highlighting that AR is the main regulator of the myofiber-type composition in fast-twitch rather than slow-twitch muscles (Hosoi et al., 2023). The enzyme-/immunohistochemical classification of myofibers was largely consistent with the expression of MyHC isoforms at the mRNA level. However, qPCR analysis showed no differences in the MyHC IIa expression between EM and SC. In pigs, Mab SC 71 binds to both isoforms of MyHC, IIa and IIx, but with different affinities (Lefaucheur et al., 2002). This could explain the difficulty in classifying the subset of myofibers expressing both MyHC isoforms, IIa and IIx, in different proportions and may also hinder detecting differences in MyHC IIa expression by qPCR when using homogenized muscle samples. Additionally, when EM was compared to SC, SSC type I myofibers from SC displayed reduced SDH activity, which might be consistent with DEGs that are enriched in the AMPK pathway (Kjøbsted et al., 2018). Although we carefully controlled the incubation time and thickness of the cryosections, which can influence the quantitative evaluation of SDH activity, caution in interpretation is still necessary.

In contrast, the effect of the short-term deprivation of testicular hormones through immunocastration was primarily observed in SSC, and was manifested by a substantial decrease of up to 20% in the CSA of slow-twitch type I oxidative myofibers compared with that in both EM and SC. A similar trend was observed in LD; however, it was not statistically significant. Previous study on the effects of immunocastration on porcine histomorphometric myofiber traits reported a lower proportion of IIb myofibers in LD of IC than in SC and a tendency towards a greater relative area occupied by IIa myofibers (Li et al., 2015). Our results for LD showed a comparable pattern, although the difference was not statistically significant. Note that the study by Li et al. (2015) did not include data on oxidative muscles or EMs. The effect of immunocastration on the histomorphometric traits of slow-twitch type I oxidative myofibers, but not on the contractile phenotype (proportion of myofibers) or *MyHC* expression aligns with data on AR-knockout male mice (MacLean et al., 2008) and the sensitivities of types I and II myofibers to testosterone treatment in healthy men (Sinha-Hikim et al., 2002). The population of satellite cells is greater in myofibers with a high oxidative potential than in those with a lower oxidative capacity (van Wessel et al., 2010), thus supporting the observed decrease in the CSA of type I myofibers in SSC in IC compared with in EM, but not in SC. Interestingly, neither qPCR nor RNA-Seq revealed significant changes in the *AR* and *ERα* expression among the studied muscles and sex categories. Comparable expression levels of *AR* have also been reported in mixed, fast- and slow-twitch hindlimb muscles of male mice (Rana et al., 2014). Therefore, the histomorphological observations raised uncertainties over which mechanisms sustain myofiber size under conditions of long-term androgen withdrawal (SC) and which mechanisms underlie muscle-specific histomorphometric traits. Research findings obtained with AR knockout male mice revealed that the key mechanisms through which androgens exert anabolic actions are the regulation of genes governing myoblast proliferation and differentiation (MacLean et al., 2008), and the suppression of myogenin/ubiquitin ligase-mediated atrophy pathways in adult muscles (Rana et al., 2014). qPCR and RNA-Seq, together with subsequent GO enrichment and KEGG pathway analysis of the DEGs, provided possible explanations for muscle-specific responses linked to the male sex category. Key genes associated with skeletal muscle tissue development and cell differentiation, such as *ankyrin repeat domain 11* (*ANKRD1*), *kelch-like family member 40, early growth response 1* (*EGR1*), and *activating transcription factor 3* (*ATF3*), were downregulated in LD in EM but not in SC. Interestingly, comparison of the EM LD transcriptome with that in IC also revealed the downregulation of genes related to skeletal muscle development and differentiation, including *ANKRD1, EGR1, ATF3, JunB Proto-Oncogene* (*JUNB*), *BTG anti-proliferation factor 2* (*BTG2*), and *crystallin alpha B* (*CRYAB*). These genes were previously identified as functional candidates for skeletal muscle development in domestic animals (reviewed in Mohammadabadi, Bordbar, Jensen, Du and Guo (2021)). This suggests that LD adapts to short- and long-term androgen deficiency by upregulating genes governing myoblast proliferation and differentiation, thereby maintaining the myofiber size. In the SC, the transition of satellite cells from a proliferative to a quiescent state may not have been initiated because of the lack of androgens from the neonatal period onwards (Seo et al., 2019). Notably, the IC group we previously showed testosterone concentrations comparable to those in the EM group up to 22 weeks of age (Kress et al., 2020). A sharp decline in testosterone levels in puberty, confirmed experimentally two weeks after the second vaccination at 24 weeks of age (Kress et al., 2020), could indicate a potential hindrance to the successful transition of satellite cells from a proliferative to a quiescent state or alternatively, a transition from quiescent to proliferative states. The upregulated expression of *myoclin* (*MYOC*) in LD in SC and IC compared with that in EM could also contribute to the maintenance of the muscle size in the absence of a positive effect of androgens because its role in the regulation of the muscle size is supported by the muscle hypertrophy phenotype observed in transgenic mice overexpressing *MYOC* (reviewed in Schiaffino, Reggiani, Akimoto and Blaauw (2021)). In addition, a gene associated with adipogenesis, *AT-rich interaction domain 5B* (*ARID5B)*, was downregulated in LD in EM compared with in IC. Muscle-specific deletion of *ARID5B* in mice affects fuel utilization in skeletal muscles, favoring fatty

acids for energy generation (Murray, Ehsani, Najjar, Zhang & Itakura, 2022) and increased *ARID5B* expression could contribute to the reported metabolic changes in the IC (Batorek-Lukač, Dubois, Noblet, Čandek-Potokar & Labussière, 2016; Poklukar et al., 2021). Therefore, further investigations are required to reveal its potential involvement in metabolic changes in the IC. In addition, in LD in IC, DEGs were enriched in p53 signaling (*THBS1, SERPINE1*) and ECM-receptor interaction pathways (*THBS1, SPP1*) compared with in SC. The increased expression of *SERPINE1*, confirmed also by qPCR can be induced by hormones like insulin-like growth factor-1 (IGF-1), which aligns with substantially higher serum IGF-1 levels reported in IC compared with SC (Fernández-Fígares et al., 2023). The increased expression of both *SERPINE1* and the profibrotic gene *THBS1* can also underlie the increase in the collagen content, as previously reported in LD in IC compared with in SC (Škrlep et al., 2020). The role of *SPP1* (also known as *osteopontin*), a p53-target gene, in determining skeletal muscle size remains unclear (Pagel, Wasgewatte Wijesinghe, Taghavi Esfandouni & Mackie, 2014).

Interestingly, the oxidative SSC responded differently to short-term androgen deprivation induced by immunocastration and displayed distinctive transcriptome profiles. The reduced CSA of type I myofibers in SSC in IC, compared with EM and SC, most likely results from increased muscle protein degradation. This is supported by the increased expression of the ubiquitin ligases *TRIM63* and FBXO32 in SSC in IC compared with in SC, whereas the levels of both atrophy marker genes (*TRIM63* and *FBXO32*) in IC and EM were comparable. The suppression of the ubiquitin ligase-mediated atrophy pathways in SC aligns with the preservation of muscle mass after *AR* ablation (Hosoi et al., 2023). In contrast, in SSC in IC, short-term androgen deprivation caused an imbalance in protein homeostasis, increasing protein degradation via the ubiquitin-proteasome signaling pathway without counterbalancing the effect of androgens on the *de novo* protein synthesis seen in EM. Supporting the latter, surgical castration in adult mice suppresses myofibrillar protein synthesis (White et al., 2013). Further, DEGs involved in transcriptional misregulation in cancer were enriched in SSC, with *CEBPB* and *NR4A3* identified as candidate genes. Promoters of *TRIM63* and *FBX032* exhibit putative binding for different transcription factors including *CEBPB*, which activate either *TRIM63* or *FBX032* individually or in combination with other transcription factors (Bodine & Baehr, 2014), whereas differences in *NR4A3* expression can be linked to the regulation of genes and pathways related to adiposity, skeletal muscle metabolic and oxidative capacity, and glucose utilization and storage (Pearen et al., 2013). Comparing EM to SC revealed DEGs enriched in the AMPK signaling pathway, implicating two candidate genes (*PGC-1α* and *SCD*) in modulating energy expenditure and lean muscle phenotype.

The AMPK pathway modulates anabolic and catabolic pathways and regulates mitochondrial biogenesis through *PGC-1α* (Kjøbsted et al., 2018). RNA-Seq data for *PGC-1α* were consistent with previously reported testosterone-promoted increases in *PGC-1α* expression in the skeletal muscle (Usui et al., 2014). Unfortunately, due to large differences between individual animals within experimental groups, the *PGC-1α* RNASeq data were not confirmed by qPCR. High individual variations in *PGC-1α* expression were also observed in our previous studies (Fazarinc et al., 2020; Vrecl et al., 2018). SCD-deficient mice (Dobrzyń & Dobrzyń, 2006) displayed increased energy expenditure and reduced body adiposity due to the upregulation of fatty acid oxidation genes. Therefore, lower expression of *SCD* in the skeletal muscles in EM may contribute to their leaner phenotype. *SCD* expression levels also correlate with the IMF content and meat quality in pigs (reviewed in Yan, Guo and Yin, 2023). Finally, DEGs (*PGC-1α, HK2, PRKAG2*, and *FOXO1*) were enriched in the insulin signaling pathway when comparing SSC in IC with that in SC. Transgenic mice overexpressing *FOXO1* in the skeletal muscle show a negative regulation of muscle mass through increased protein degradation and reduced expression of genes related to slow-twitch type I myofibers (Kamei et al., 2004). Our RNA-Seq and qPCR data also provide evidence of increased protein degradation via upregulated ubiquitin ligases (*TRIM63* and *FOX32*) in the IC. The observed decrease in the CSA of type I myofibers in SSC in IC might align with the negative effect of *FOXO1* expression on the level of structural proteins specific to slow-twitch type I myofibers (Kamei et al., 2004). All identified genes (*PGC-1α, HK2*, and *PRKAG2*) play roles in cellular energy homeostasis; therefore, their regulation may contribute to the reported metabolic changes in IC (Batorek-Lukač et al., 2016; Poklukar et al., 2021). Increased expression of the glycolytic enzyme *HK2* in SSC of IC compared with SC may align with the findings of the upregulation of enzymes involved in carbohydrate metabolism in aging slow-twitch type I myofibers of male humans (Murgia et al., 2017) or alternatively, increased *HK2* expression may act as a compensatory mechanism to preserve amino acids for protein synthesis; however, this was suggested to be an AR-related change (Sakakibara et al., 2021).

5. Conclusions

This study demonstrated that different hormonal statuses associated with the method of castration exert muscle-specific effects on histomorphometric traits and transcriptome profiles. Long-term androgen deficiency (related to surgical castration) affects the proportion of fast-twitch type IIa myofibers in LD, aligning with the role of androgens in supporting the fast-twitch phenotype. Conversely, short-term androgen deprivation (i.e., immunocastration) primarily affects the histomorphometric properties of oxidative type I myofibers in SSC. The transcriptome profiles obtained here supported the observed muscle-specific histomorphometric traits. RNA-Seq data suggested that glycolytic LD adapts to androgen deprivation by upregulating genes that control myoblast proliferation and differentiation, such as ANKRD1, EGR1, and ATF3, thereby preserving myofiber size. In contrast, the reduction in the CSA of SSC oxidative type I myofibers in IC pigs suggests an increase in muscle protein degradation through the ubiquitin ligase-mediated atrophy pathway (increased expression of TRIM63 and FBXO32). Simultaneously, the observed myofiber type-specific effect might be attributed to upregulated FOXO1. Because our analysis was mainly focused on gene expression at the transcriptomic level, possible post-translational effects of sex hormones could not be detected; thus, further observations at the protein level need to be conducted. Finally, the potential candidate genes (HK2, ARID5B, SERPINE1, and SCD) identified in IC may be linked to specific metabolic and meat quality traits. This provides a basis for further studies on the effects of immunocastration on porcine skeletal myofibers and carcass/meat quality traits, with potential implications for agricultural practices.

Funding

The authors received financial support from the EC and Slovenian Ministry for Agriculture in the framework of ERA NET SusAn SuSi (631–10/2015/7; sustainability in pork production with immunocastration). The authors also acknowledge financial support from the Slovenian Research and Innovation Agency programs P4-0133 (N.B.-L., K.P., M.Š., M.Č.-P.) and P4-0053 (G.F. and M.V.).

Data availability statements

The datasets used and/or analyzed in the current study are available from the corresponding author upon reasonable request. The RNA-Seq data that support the findings of this study were submitted to the NCBI Gene Expression Omnibus (GEO; Bethesda, MD, USA) under GEO accession number GSE183240.

Consent to publish

Not applicable.

Ethics approval and consent to participate

This study was approved by the Ethical Committee for Animal Experiments at the regional level by the authority of Tübingen, Germany (permission for animal experimentation ID: HOH 47/17TH). The Institute of Preclinical Sciences, Veterinary faculty of the University of Ljubljana and the Agricultural Institute of Slovenia were approved by the Veterinary Administration of the Republic of Slovenia for the use of animal by-products C1 and 2 (category 1 and 2 1069/2009/ES) for research purposes (permits No. SI B 07-22-07 and No. SI B 07-22-49, respectively).

CRediT authorship contribution statement

Klavdija Poklukar: Writing – review & editing, Methodology, Investigation. **Anja Erbežnik:** Writing – review & editing, Methodology, Investigation. **Gregor Fazarinc:** Writing – review & editing, Writing – original draft, Methodology, Investigation. **Kevin Kress:** Writing – review & editing, Investigation. **Nina Batorek-Lukač:** Writing – review & editing, Methodology, Investigation. **Martin Škrlep:** Writing – review & editing, Methodology, Investigation. **Volker Stefanski:** Writing – review & editing, Funding acquisition. **Marjeta Čandek-Potokar:** Writing – review & editing, Supervision, Project administration, Methodology, Funding acquisition, Conceptualization. **Milka Vrecl:** Writing – review & editing, Writing – original draft, Supervision, Project administration, Methodology, Investigation, Funding acquisition, Conceptualization.

Declaration of competing interest

The authors declare that they have no known competing financial interests or personal relationships that could have appeared to influence the work reported in this paper.

Acknowledgments

The results of this study were accomplished within the SuSI project co-financed by Susan EraNet and the Slovenian Ministry of Agriculture, Forestry, and Food. Collaboration within the COST action CA12215 IPEMA and core financing from the Slovenian Research and Innovation Agency (grants P4-0133 and P4-0053, PhD scholarship for KP) are also acknowledged. We would also like to thank Magdalena Dobravec and Jasna Šporar for excellent technical support.

Supplementary materials

Supplementary material associated with this article can be found, in the online version, at doi:10.1016/j.vas.2024.100383.

References

Aluwé, M., Heyrman, E., Almeida, J. M., Babol, J., Battacone, G., Čítek, J., Font, I. F. M., Getya, A., Karolyi, D., Kostyra, E., Kress, K., Kušec, G., Mörlein, D., Semenova, A., Škrlep, M., Stoyanchev, T., Tomašević, I., Tudoreanu, L., Van Son, M., Żakowska-Biemans, S., Zamaratskaia, G., Van den Broeke, A., & Egea, M. (2020). Exploratory survey on European consumer and stakeholder attitudes towards alternatives for surgical castration of piglets. *Animals, 10*. https://doi.org/10.3390/ani10101758. Article 1758.

Batorek, N., Čandek-Potokar, M., Bonneau, M., & Van Milgen, J. (2012). Meta-analysis of the effect of immunocastration on production performance, reproductive organs and boar taint compounds in pigs. *Animals, 6*, 1330–1338. https://doi.org/10.1017/S1751731112000146

Batorek-Lukač, N., Dubois, S., Noblet, J., Čandek-Potokar, M., & Labussière, E. (2016). Effect of high dietary fat content on heat production and lipid and protein deposition in growing immunocastrated male pigs. *Animals, 10*, 1941–1948. https://doi.org/10.1017/S1751731116000719

Batorek-Lukač, N., Kress, K., Čandek-Potokar, M., Fazarinc, G., Škrlep, M., Poklukar, K., Wesoly, R., Stefanski, V., & Vrecl, M. (2022). Immunocastration in adult boars as a model for late-onset hypogonadism. *Andrology, 10*, 1217–1232. https://doi.org/10.1111/andr.13219

Bodine, S. C., & Baehr, L. M. (2014). Skeletal muscle atrophy and the E3 ubiquitin ligases MuRF1 and MAFbx/atrogin-1. *American Journal of Physiology - Endocrinology and Metabolism, 307*, E469–E484. https://doi.org/10.1152/ajpendo.00204.2014

Bonneau, M., & Weiler, U. (2019). Pros and cons of alternatives to piglet castration: welfare, boar taint, and other meat quality traits. *Animals, 9*. https://doi.org/10.3390/ani9110884. Article 884.

Borell, E. V., Bonneau, M., Holinger, M., Prunier, A., Stefanski, V., Zöls, S., & Weiler, U. (2020). Welfare aspects of raising entire male pigs and immunocastrates. Animals, 10, Article 2140. https://doi.org/10.3390/ani10112140.

Daszkiewicz, T., Bąk, T., & Denaburski, J. (2005). Quality of pork with a different intramuscular fat (IMF) content. *Polish Journal of Food and Nutrition Sciences, 55*, 31–36.

Dobrzyń, A., & Dobrzyń, P. (2006). Stearoyl-CoA desaturase–a new player in skeletal muscle metabolism regulation. *Journal of Physiology and Pharmacology, 57*, 31–42.

Doumit, M. E., Cook, D. R., & Merkel, R. A. (1996). Testosterone up-regulates androgen receptors and decreases differentiation of porcine myogenic satellite cells in vitro. *Endocrinology, 137*, 1385–1394. https://doi.org/10.1210/endo.137.4.8625915

Dubois, V., Laurent, M. R., Sinnesael, M., Cielen, N., Helsen, C., Clinckemalie, L., Spans, L., Gayan-Ramirez, G., Deldicque, L., Hespel, P., Carmeliet, G., Vanderschueren, D., & Claessens, F. (2014). A satellite cell-specific knockout of the androgen receptor reveals myostatin as a direct androgen target in skeletal muscle. *The FASEB Journal, 28*, 2979–2994. https://doi.org/10.1096/fj.14-249748

Dubois, V., Laurent, M., Boonen, S., Vanderschueren, D., & Claessens, F. (2012). Androgens and skeletal muscle: cellular and molecular action mechanisms underlying the anabolic actions. *Cellular and Molecular Life Sciences, 69*, 1651–1667. https://doi.org/10.1007/s00018-011-0883-3

Eriksson, A., Kadi, F., Malm, C., & Thornell, L. E. (2005). Skeletal muscle morphology in power-lifters with and without anabolic steroids. *Histochemistry and Cell Biology, 124*, 167–175. https://doi.org/10.1007/s00418-005-0029-5

Erkens, T., Van Poucke, M., Vandesompele, J., Goossens, K., Van Zeveren, A., & Peelman, L. J. (2006). Development of a new set of reference genes for normalization of real-time RT-PCR data of porcine backfat and longissimus dorsi muscle, and evaluation with PPARGC1A. *BMC Biotechnology, 6*. https://doi.org/10.1186/1472-6750-6-41. Article 41.

Fazarinc, G., Batorek-Lukač, N., Škrlep, M., Poklukar, K., Van den Broeke, A., Kress, K., Labussière, E., Stefanski, V., Vrecl, M., & Čandek-Potokar, M. (2023). Male reproductive organ weight: criteria for detection of androstenone-positive carcasses in immunocastrated and entire male pigs. *Animals, 13*. https://doi.org/10.3390/ani13122042. Article 2042.

Fazarinc, G., Vrecl, M., Poklukar, K., Škrlep, M., Batorek-Lukač, N., Brankovič, J., Tomažin, U., & Čandek-Potokar, M. (2020). Expression of myosin heavy chain and some energy metabolism-telated genes in the longissimus dorsi muscle of Krškopolje pigs: effect of the production system. In *Frontiers in Veterinary Science, 7*. https://doi.org/10.3389/fvets.2020.533936. Article 533936 View at publisher Google Scholar.

Fazarinc, G., Vrecl, M., Škorjanc, D., Čehovin, T., & Čandek-Potokar, M. (2017). Dynamics of myosin heavy chain isoform transition in the longissimus muscle of domestic and wild pigs during growth: a comparative study. *Animal, 11*, 164–174. https://doi.org/10.1017/S1751731116001312

Fernández-Fígares, I., Haro, A., Lachica, M., Lara, L., Seiquer, I., & Nieto, R. (2023). Metabolic profile of growing immune- and surgically castrated Iberian pigs fed diets of different amino acid concentration. Animals, 13, Article 2650. https://doi.org/10.3390/ani13162650.

Fernandez, X., Lefaucheur, L., & Čandek, M. (1995). Comparative study of two classifications of muscle fibres: consequences for the photometric determination of glycogen according to fibre type in red and white muscle of the pig. *Meat Science, 41*, 225–235. https://doi.org/10.1016/0309-1740(94)00059-G

Fiedler, I., Ender, K., Wicke, M., Maak, S., Lengerken, G. V., & Meyer, W. (1999). Structural and functional characteristics of muscle fibres in pigs with different malignant hyperthermia susceptibility (MHS) and different meat quality. *Meat Science, 53*, 9–15. https://doi.org/10.1016/S0309-1740(99)00030-3

Haizlip, K. M., Harrison, B. C., & Leinwand, L. A. (2015). Sex-based differences in skeletal muscle kinetics and fiber-type composition. *Physiology, 30*, 30–39. https://doi.org/10.1152/physiol.00024.2014

Hosoi, T., Yakabe, M., Sasakawa, H., Sasako, T., Ueki, K., Kato, S., Tokuoka, S. M., Oda, Y., Abe, M., Matsumoto, T., Akishita, M., & Ogawa, S. (2023). Sarcopenia phenotype and impaired muscle function in male mice with fast-twitch muscle-specific knockout of the androgen receptor. *Proceedings of the National Academy of Sciences, 120*. https://doi.org/10.1073/pnas.2218032120. Article e2218032120.

Kalbe, C., Mau, M., Wollenhaupt, K., & Rehfeldt, C. (2007). Evidence for estrogen receptor alpha and beta expression in skeletal muscle of pigs. *Histochemistry and Cell Biology, 127*, 95–107. https://doi.org/10.1007/s00418-006-0224-z

Kamei, Y., Miura, S., Suzuki, M., Kai, Y., Mizukami, J., Taniguchi, T., Mochida, K., Hata, T., Matsuda, J., Aburatani, H., Nishino, I., & Ezaki, O. (2004). Skeletal muscle FOXO1 (FKHR) transgenic mice have less skeletal muscle mass, down-regulated Type I (slow twitch/red muscle) fiber genes, and impaired glycemic control. *The Journal of Biological Chemistry, 279*, 41114–41123. https://doi.org/10.1074/jbc.M400674200

Kjøbsted, R., Hingst, J. R., Fentz, J., Foretz, M., Sanz, M. N., Pehmøller, C., Shum, M., Marette, A., Mounier, R., Treebak, J. T., Wojtaszewski, J. F. P., Viollet, B., & Lantier, L. (2018). AMPK in skeletal muscle function and metabolism. *The FASEB Journal, 32*, 1741–1777. https://doi.org/10.1096/fj.201700442R

Ko, B., & Van Raamsdonk, J. M. (2023). RNA sequencing of pooled samples effectively identifies differentially expressed genes. *Biology, 12*. https://doi.org/10.3390/biology12060812. Article 812.

Koo, J. H., Kim, T. H., Park, S. Y., Joo, M. S., Han, C. Y., Choi, C. S., & Kim, S. G. (2017). Gα13 ablation reprograms myofibers to oxidative phenotype and enhances whole-

body metabolism. *The Journal of Clinical Investigation, 127*, 3845–3860. https://doi.org/10.1172/JCI92067
Kraemer, W. J., Ratamess, N. A., Hymer, W. C., Nindl, B. C., & Fragala, M. S. (2020). Growth hormone(s), testosterone, insulin-like growth factors, and cortisol: roles and integration for cellular development and growth with exercise. *Frontiers in Endocrinology, 11*. https://doi.org/10.3389/fendo.2020.00033. Article 33.
Kress, K., Weiler, U., Schmucker, S., Čandek-Potokar, M., Vrecl, M., Fazarinc, G., … Stefanski, V. (2020). Influence of housing conditions on reliability of immunocastration and consequences for growth performance of male pigs. *Animals, 10*. https://doi.org/10.3390/ani10010027. Article 27.
Lefaucheur, L., Ecolan, P., Plantard, L., & Gueguen, N. (2002). New insights into muscle fiber types in the pig. *Journal of Histochemistry & Cytochemistry, 50*, 719–730. https://doi.org/10.1177/002215540205000513
Lefaucheur, L., Le Dividich, J., Mourot, J., Monin, G., Ecolan, P., & Krauss, D. (1991). Influence of environmental temperature on growth, muscle and adipose tissue metabolism, and meat quality in swine. *Journal of Animal Science, 69*, 2844–2854. https://doi.org/10.2527/1991.6972844x
Lefaucheur, L., Milan, D., Ecolan, P., & Le Callennec, C. (2004). Myosin heavy chain composition of different skeletal muscles in large white and Meishan pigs. *Journal of Animal Science, 82*, 1931–1941. https://doi.org/10.2527/2004.8271931x
Li, H., Gariépy, C., Jin, Y., Font, I. F. M., Fortin, J., Rocha, L. M., & Faucitano, L. (2015). Effects of ractopamine administration and castration method on muscle fiber characteristics and sensory quality of the longissimus muscle in two Piétrain pig genotypes. *Meat Science, 102*, 27–34. https://doi.org/10.1016/j.meatsci.2014.10.027
Lin-Schilstra, L., & Ingenbleek, P. T. M. (2022). A scenario analysis for implementing immunocastration as a single solution for piglet castration. *Animals, 12*. https://doi.org/10.3390/ani12131625. Article 1625.
Lin, J., Wu, H., Tarr, P. T., Zhang, C. Y., Wu, Z., Boss, O., Michael, L. F., Puigserver, P., Isotani, E., Olson, E. N., Lowell, B. B., Bassel-Duby, R., & Spiegelman, B. M. (2002). Transcriptional co-activator PGC-1 alpha drives the formation of slow-twitch muscle fibres. *Nature, 418*, 797–801. https://doi.org/10.1038/nature00904
Lin, Y., Zhao, Y., Li, R., Gong, J., Zheng, Y., & Wang, Y. (2014). PGC-1α is associated with C2C12 myoblast differentiation. *Central European Journal of Biology, 9*, 1030–1036. https://doi.org/10.2478/s11535-014-0341-y
Listrat, A., Lebret, B., Louveau, I., Astruc, T., Bonnet, M., Lefaucheur, L., Picard, B., & Bugeon, J. (2016). How muscle structure and composition influence meat and flesh quality. *The Scientific World Journal, 2016*. https://doi.org/10.1155/2016/3182746. Article 3182746.
MacLean, H. E., Chiu, W. S., Notini, A. J., Axell, A. M., Davey, R. A., McManus, J. F., Ma, C., Plant, D. R., Lynch, G. S., & Zajac, J. D. (2008). Impaired skeletal muscle development and function in male, but not female, genomic androgen receptor knockout mice. *The FASEB Journal, 22*, 2676–2689. https://doi.org/10.1096/fj.08-105726
Matarneh, S. K., Silva, S. L., & Gerrard, D. E. (2021). New insights in muscle biology that alter meat quality. *Annual Review of Animal Biosciences, 9*, 355–377. https://doi.org/10.1146/annurev-animal-021419-083902
Men, X. M., Deng, B., Xu, Z. W., Tao, X., & Qi, K. K. (2013). Age-related changes and nutritional regulation of myosin heavy-chain composition in longissimus dorsi of commercial pigs. *Animal, 7*, 1486–1492. https://doi.org/10.1017/S1751731113000992
Mohammadabadi, M., Bordbar, F., Jensen, J., Du, M., & Guo, W. (2021). Key genes regulating skeletal muscle development and growth in farm animals. *Animals, 11*. https://doi.org/10.3390/ani11030835. Article 835.
Morgan, L., Itin-Shwartz, B., Koren, L., Meyer, J. S., Matas, D., Younis, A., Novak, S., Weizmann, N., Rapaic, O., Abu Ahmad, W., Klement, E., & Raz, T. (2019). Physiological and economic benefits of abandoning invasive surgical procedures and enhancing animal welfare in swine production. *Scientific Reports, 9*. https://doi.org/10.1038/s41598-019-52677-6. Article 16093.
Mulvaney, D. R., Marple, D. N., & Merkel, R. A. (1988). Proliferation of skeletal muscle satellite cells after castration and administration of testosterone propionate. *Proceedings of the Society for Experimental Biology and Medicine, 188*, 40–45. https://doi.org/10.3181/00379727-188-42704
Murgia, M, Toniolo, L., NNagaraj, N., Ciciliot, S., Vindigni, V., Schiaffino, S., Reggiani, C., & Mann, M. (2017). Single muscle fiber proteomics reveals fiber-type-specific features of human muscle aging. *Cell Reports, 19*, 2396–2409. https://doi.org/10.1016/j.celrep.2017.05.054
Murray, J., Ehsani, A., Najjar, L., Zhang, G., & Itakura, K. (2022). Muscle-specific deletion of Arid5b causes metabolic changes in skeletal muscle that affect adipose tissue and liver. *Frontiers in Endocrinology, 13*. https://doi.org/10.3389/fendo.2022.1083311. Article 1083311.
Nachlas, M. M., Tsou, K. C., de Souza, E., Cheng, C. S., & Seligman, A. M. (1957). Cytochemical demonstration of succinic dehydrogenase by the use of a new p-nitrophenyl substituted ditetrazole. *Journal of Histochemistry & Cytochemistry, 5*, 420–436. https://doi.org/10.1177/5.4.420
Pagel, C. N., Wasgewatte Wijesinghe, D. K., Taghavi Esfandouni, N., & Mackie, E. J. (2014). Osteopontin, inflammation and myogenesis: influencing regeneration, fibrosis and size of skeletal muscle. *Journal of Cell Communication and Signaling, 8*, 95–103. https://doi.org/10.1007/s12079-013-0217-3
Park, J., Song, S., Cheng, H., Im, C., Jung, E. Y., Moon, S. S., Choi, J., Hur, S. J., Joo, S. T., & Kim, G. D. (2022). Comparison of meat quality and muscle fiber characteristics between porcine skeletal muscles with different architectures. *Food Science of Animal Resources, 42*, 874–888. https://doi.org/10.5851/kosfa.2022.e40
Pauly, C., Luginbühl, W., Ampuero, S., & Bee, G. (2012). Expected effects on carcass and pork quality when surgical castration is omitted—Results of a meta-analysis study. *Meat Science, 92*, 858–862. https://doi.org/10.1016/j.meatsci.2012.06.007
Pearen, M. A., Goode, J. M., Fitzsimmons, R. L., Eriksson, N. A., Thomas, G. P., Cowin, G. J., Wang, S. C., Tuong, Z. K., & Muscat, G. E. (2013). Transgenic muscle-specific Nor-1 expression regulates multiple pathways that effect adiposity, metabolism, and endurance. *Molecular Endocrinology, 27*, 1897–1917. https://doi.org/10.1210/me.2013-1205
Pellegrino, M. A., Canepari, M., Rossi, R., D'Antona, G., Reggiani, C., & Bottinelli, R. (2003). Orthologous myosin isoforms and scaling of shortening velocity with body size in mouse, rat, rabbit and human muscles. *Journal of Physiology, 546*, 677–689. https://doi.org/10.1113/jphysiol.2002.027375
Poklukar, K., Čandek-Potokar, M., Vrecl, M., Batorek-Lukač, N., Fazarinc, G., Kress, K., Weiler, U., Stefanski, V., & Škrlep, M. (2021). The effect of immunocastration on adipose tissue deposition and composition in pigs. *Animal, 15*. https://doi.org/10.1016/j.animal.2020.100118. Article 100118.
Poklukar, K., Čandek-Potokar, M., Vrecl, M., Batorek-Lukač, N., Fazarinc, G., Kress, K., Stefanski, V., & Škrlep, M. (2021). Adipose tissue gene expression of entire male, immunocastrated and surgically castrated pigs. *International Journal of Molecular Sciences, 22*. https://doi.org/10.3390/ijms22041768. Article 1768.
Rana, K., Lee, N. K., Zajac, J. D., & MacLean, H. E. (2014). Expression of androgen receptor target genes in skeletal muscle. *Asian Journal of Andrology, 16*, 675–683. https://doi.org/10.4103/1008-682X.122861
Rossetti, M. L., & Gordon, B. S. (2017). The role of androgens in the regulation of muscle oxidative capacity following aerobic exercise training. *Applied Physiology, Nutrition, and Metabolism, 42*, 1001–1007. https://doi.org/10.1139/apnm-2017-0230
Sakakibara, I., Yanagihara, Y., Himori, K., Yamada, T., Sakai, H., Sawada, Y., Takahashi, H., Saeki, N., Hirakawa, H., Yokoyama, A., Fukada, S. I., Sawasaki, T., & Imai, Y. (2021). Myofiber androgen receptor increases muscle strength mediated by a skeletal muscle splicing variant of Mylk4. *iScience, 24*. https://doi.org/10.1016/j.isci.2021.102303. Article 102303.
Schiaffino, S., Gorza, L., Sartore, S., Saggin, L., Ausoni, S., Vianello, M., Gundersen, K., & Lomo, T. (1989). Three myosin heavy chain isoforms in type 2 skeletal muscle fibres. *Journal of Muscle Research & Cell Motility, 10*, 197–205. https://doi.org/10.1007/BF01739810
Schiaffino, S., Reggiani, C., Akimoto, T., & Blaauw, B. (2021). Molecular mechanisms of skeletal muscle hypertrophy. *Journal of Neuromuscular Diseases, 8*, 169–183. https://doi.org/10.3233/JND-200568
Seo, J. Y., Kim, J. H., & Kong, Y. Y. (2019). Unraveling the paradoxical action of androgens on muscle stem cells. *Molecules and Cells, 42*, 97–103. https://doi.org/10.14348/molcells.2019.0004
Sinha-Hikim, I., Artaza, J., Woodhouse, L., Gonzalez-Cadavid, N., Singh, A. B., Lee, M. I., Storer, T. W., Casaburi, R., Shen, R., & Bhasin, S. (2002). Testosterone-induced increase in muscle size in healthy young men is associated with muscle fiber hypertrophy. *American Journal of Physiology - Endocrinology and Metabolism, 283*, E154–E164. https://doi.org/10.1152/ajpendo.00502.2001
Sinha-Hikim, I., Taylor, W. E., Gonzalez-Cadavid, N. F., Zheng, W., & Bhasin, S. (2004). Androgen receptor in human skeletal muscle and cultured muscle satellite cells: up-regulation by androgen treatment. *The Journal of Clinical Endocrinology and Metabolism, 89*, 5245–5255. https://doi.org/10.1210/jc.2004-0084
Škrlep, M., Poklukar, K., Kress, K., Vrecl, M., Fazarinc, G., Batorek Lukač, N., Weiler, U., Stefanski, V., & Čandek-Potokar, M. (2020). Effect of immunocastration and housing conditions on pig carcass and meat quality traits. *Translational Animal Science, 4*. https://doi.org/10.1093/tas/txaa055. Article txaa055.
Škrlep, M., Tomašević, I., Mörlein, D., Novaković, S., Egea, M., Garrido, M. D., Linares, M. B., Peñaranda, I., Aluwé, M., & Font, I. F. M. (2020). The use of pork from entire male and immunocastrated pigs for meat products-an overview with recommendations. *Animals, 10*. https://doi.org/10.3390/ani10101754. Article 1754.
Steybe, L., Kress, K., Schmucker, S., & Stefanski, V. (2021). Impact of housing condition on welfare and behavior of immunocastrated fattening pigs (*Sus scrofa domestica*). Animals, 11, Article 618. https://doi.org/10.3390/ani11030618.
Usui, T., Kajita, K., Kajita, T., Mori, I., Hanamoto, T., Ikeda, T., Okada, H., Taguchi, K., Kitada, Y., Morita, H., Sasaki, T., Kitamura, T., Sato, T., Kojima, I., & Ishizuka, T. (2014). Elevated mitochondrial biogenesis in skeletal muscle is associated with testosterone-induced body weight loss in male mice. *FEBS Letters, 588*, 1935–1941. https://doi.org/10.1016/j.febslet.2014.03.051
van Wessel, T., de Haan, A., van der Laarse, W. J., & Jaspers, R. T. (2010). The muscle fiber type-fiber size paradox: hypertrophy or oxidative metabolism? *European Journal of Applied Physiology, 110*, 665–694. https://doi.org/10.1007/s00421-010-1545-0
Vrecl, M., Cotman, M., Uršič, M., Čandek-Potokar, M., & Fazarinc, G. (2018). Age-dependent expression of MyHC isoforms and lipid metabolism-related genes in the longissimus dorsi muscle of wild and domestic pigs. *Animals, 9*. https://doi.org/10.3390/ani9010010. Article 10.
Walter, W., Sánchez-Cabo, F., & Ricote, M. (2015). GOplot: an R package for visually combining expression data with functional analysis. *Bioinformatics, 31*, 2912–2914. https://doi.org/10.1093/bioinformatics/btv300
Werner, D., Baldinger, L., Bussemas, R., Büttner, S., Weißmann, F., Ciulu, M., Mörlein, J., & Mörlein, D. (2021). Early immunocastration of pigs: from farming to meat quality. *Animals, 11*. https://doi.org/10.3390/ani11020298. Article 298.
White, J. P., Gao, S., Puppa, M. J., Sato, S., Welle, S. L., & Carson, J. A. (2013). Testosterone regulation of Akt/mTORC1/FoxO3a signaling in skeletal muscle. *Molecular and Cellular Endocrinology, 365*, 174–186. https://doi.org/10.1016/j.mce.2012.10.019
Wimmers, K., Ngu, N. T., Jennen, D. G., Tesfaye, D., Murani, E., Schellander, K., & Ponsuksili, S. (2008). Relationship between myosin heavy chain isoform expression and muscling in several diverse pig breeds. *Journal of Animal Science, 86*, 795–803. https://doi.org/10.2527/jas.2006-521

Yan, E., Guo, J., & Yin, J. (2023). Nutritional regulation of skeletal muscle energy metabolism, lipid accumulation and meat quality in pigs. *Animal Nutrition, 14*, 185–192. https://doi.org/10.1016/j.aninu.2023.04.009

Young, M. D., Wakefield, M. J., Smyth, G. K., & Oshlack, A. (2010). Gene ontology analysis for RNA-seq: accounting for selection bias. *Genome Biology*, 11. https://doi.org/10.1186/gb-2010-11-2-r14. Article R14.

Zhang, C., Luo, J. Q., Zheng, P., Yu, B., Huang, Z. Q., Mao, X. B., He, J., Yu, J., Chen, J. L., & Chen, D. W. (2015). Differential expression of lipid metabolism-related genes and myosin heavy chain isoform genes in pig muscle tissue leading to different meat quality. *Animal, 9*, 1073–1080. https://doi.org/10.1017/S1751731115000324